

# Deepening subwavelength acoustic resonance via metamaterials with universal broadband elliptical microstructure

Cite as: Appl. Phys. Lett. **112**, 251902 (2018); <https://doi.org/10.1063/1.5022197>

Submitted: 11 January 2018 . Accepted: 10 April 2018 . Published Online: 18 June 2018

William D. Rowley, William J. Parnell , I. David Abrahams, S. Ruth Voisey, John Lamb, and Nicolas Etaix



View Online



Export Citation



CrossMark

## ARTICLES YOU MAY BE INTERESTED IN

[Acoustic metasurface-based perfect absorber with deep subwavelength thickness](#)

Applied Physics Letters **108**, 063502 (2016); <https://doi.org/10.1063/1.4941338>

[Perspective: Acoustic metamaterials in transition](#)

Journal of Applied Physics **123**, 090901 (2018); <https://doi.org/10.1063/1.5007682>

[Acoustic perfect absorption and broadband insulation achieved by double-zero metamaterials](#)

Applied Physics Letters **112**, 021901 (2018); <https://doi.org/10.1063/1.5018180>



Lock-in Amplifiers

Zurich Instruments

Watch the Video 

# Deepening subwavelength acoustic resonance via metamaterials with universal broadband elliptical microstructure

William D. Rowley,<sup>1,a)</sup> William J. Parnell,<sup>1,b)</sup> I. David Abrahams,<sup>2,c)</sup> S. Ruth Voisey,<sup>3,d)</sup> John Lamb,<sup>3,e)</sup> and Nicolas Etaix<sup>3,f)</sup>

<sup>1</sup>*School of Mathematics, University of Manchester, Oxford Road, Manchester M13 9PL, United Kingdom*

<sup>2</sup>*Isaac Newton Institute, University of Cambridge, 20 Clarkson Road, Cambridge CB3 0EH, United Kingdom*

<sup>3</sup>*Dyson Technology Limited, Tetbury Hill, Malmesbury SN16 0RP, United Kingdom*

(Received 11 January 2018; accepted 10 April 2018; published online 18 June 2018)

Slow sound is a frequently exploited phenomenon that metamaterials can induce in order to permit wave energy compression, redirection, imaging, sound absorption, and other special functionalities. Generally, however, such slow sound structures have a poor impedance match to air, particularly at low frequencies and consequently exhibit strong transmission only in narrow frequency ranges. This therefore strongly restricts their application in wave manipulation devices. In this work, we design a slow sound medium that halves the effective speed of sound in air over a wide range of low frequencies (hence our referral to the microstructure as “broadband”), whilst simultaneously maintaining a near impedance match to air. This is achieved with a rectangular array of acoustically rigid cylinders of elliptical cross section, a microstructure that is motivated by combining transformation acoustics with homogenization. Microstructural parameters are optimized in order to provide the required anisotropic material properties as well as near impedance matching. We then employ this microstructure in order to halve the size of a quarter-wavelength resonator (QWR) or equivalently to halve the resonant frequency of a QWR of a given size. This provides significant space savings in the context of low-frequency tonal noise attenuation in confined environments where the absorbing material is adjacent to the region in which sound propagates, such as in a duct. We employ the term “universal” since we envisage that this microstructure may be employed in a number of diverse applications involving sound manipulation. © 2018 Author(s). All article content, except where otherwise noted, is licensed under a Creative Commons Attribution (CC BY) license (<http://creativecommons.org/licenses/by/4.0/>). <https://doi.org/10.1063/1.5022197>

The ability to shape, redirect, and manipulate sound has been of interest for many decades, and the recent emergence of metamaterials and complex composites has driven this area forward with a multitude of exciting results including cloaking, negative refraction, and lensing.<sup>1–7</sup> The application of slow sound via space-coiling, labyrinthine type structures,<sup>8–11</sup> and helical devices<sup>12</sup> is of significant interest since, as with slow light, the concept has great promise in a number of scenarios. In many applications however, when the surrounding material is air, one requires full, broadband transmission through slow sound devices in order to enable complete manipulation of the sound field via a metamaterial. This is not the case in general for previously developed materials.<sup>9,12,13</sup>

In this letter, we use the method of transformation acoustics<sup>14,15</sup> to design a medium in which space is apparently stretched or alternatively sound is effectively slowed, whilst also ensuring that the medium is almost-impedance matched to air. We employ a recently developed homogenization method<sup>16,17</sup> in order to realise this material via a microstructure consisting of rigid elliptical cylinders

arranged in a rectangular array. The explicit form of anisotropic density provided via the homogenization scheme means that microstructures can be optimised to the best effect. This microstructure may be contrasted with perforated plates, which have been the focus of the majority of previous studies and have been employed to realise cloaks,<sup>18</sup> ground cloaks,<sup>19,20</sup> lensing,<sup>5</sup> and right angle bend transformations.<sup>21</sup> The newly proposed elliptical microstructure achieves a near impedance match to air in a broad range of low frequencies and furthermore induces an effective sound speed in the heterogeneous medium that can be reduced to one half that of air. These achievements and generalizations of the microstructure can be exploited in a number of important applications and therefore we term the microstructure “universal.” Furthermore, since the lengthscale of the microstructure is much less than that of the propagating wavelength, it is also a “broadband” material that can be employed in a wide range of low frequency applications where this lengthscale separation holds. Here, we focus on the application of low-frequency resonance and exploit our findings to halve the size of the well known quarter-wavelength resonator (QWR).<sup>22</sup> A QWR is a side branch of an acoustic duct used to attenuate tonal noise of wavelength approximately four times the length of the side branch; this attenuation is achieved through destructive interference. Theoretical predictions of the resonant frequency are validated experimentally; the resonance peak is shifted close to that

<sup>a)</sup>Electronic mail: william.rowley-3@postgrad.manchester.ac.uk

<sup>b)</sup>Electronic mail: William.Parnell@manchester.ac.uk

<sup>c)</sup>Electronic mail: i.d.abrahams@newton.ac.uk

<sup>d)</sup>Electronic mail: Ruth.Voisey@dyson.com

<sup>e)</sup>Electronic mail: John.Lamb@dyson.com

<sup>f)</sup>Electronic mail: Nicolas.Etaix@dyson.com

predicted by the theory, associated with the reduction in sound speed in the resonator. The amplitude of the resonance is reduced somewhat due to the small impedance mismatch between air and the metamaterial and also the inherent viscous and thermal effects in the heterogeneous structure, but the ability to significantly reduce the resonant frequency (or equivalently reduce the size of the resonator) is undoubtedly of significant practical importance.

More broadly speaking, along with Helmholtz resonators and Herschel-Quincke tubes, QWRs are frequently used in applications where low-frequency tonal noise needs to be attenuated in a confined environment such as a duct. Attenuating acoustic waves in such contexts where sound propagates orthogonal to the walls of the confined region is traditionally very difficult. Although high-frequency sound can easily be attenuated via standard sound-absorbing foams, low-frequency sound is more difficult to attenuate since it requires prohibitively large amounts of such materials. The standard approach for low-frequency sound attenuation in ducts is therefore to employ resonators and side-branches<sup>23,24</sup> and although such side branch resonators can be useful, their size frequently prohibits practical use, although some work has been done using standard resonators in sequence.<sup>23–25</sup> Generally, there is a lack of work in the area of metamaterial approaches applied to sound attenuation in confined spaces; furthermore, the resonators employed would often impede flow.<sup>26</sup> This is in contrast to sound absorption in free-space where sound is incident onto a surface: the concept of metasurfaces has received significant attention, with many works describing structures capable of perfect sound absorption at low-frequency.<sup>27,28</sup> Unfortunately, this concept cannot be of use in the same manner in the context of propagation in confined regions, since the metasurface would either sit across the duct, orthogonal to the direction of the sound field, perform well but obstruct flow, or sit parallel to the direction of sound, and be ineffective, whilst permitting flow. The requirement to allow for air flow in the duct is important in many practical applications. The size restriction associated with side-branch resonators means therefore that the finding presented in this letter could be of broad significance in low-frequency noise control.

As described above, a range of necessary material properties derived through transformation acoustics have been realised in a variety of metamaterial applications and have been experimentally verified to be a good effect. Here, an effective elongation of space is provided by employing one of the simplest mappings in the theory of transformation acoustics. The transformation from the virtual primed coordinate system  $(x', y', z')$  onto the physical system  $(x, y, z)$  is  $x = x', y = \alpha y', z = \beta z'$ . We are interested in sound propagation in the two-dimensional  $xy$ -plane, with  $\alpha < 1$ , which creates an apparent elongation of space via an effective reduction in the sound speed [see Fig. 1(a)]. The microstructure will subsequently be chosen in order to realise this scenario. The parameter  $\beta$  is employed here to optimise impedance matching to air whilst still permitting realistic microstructures.

With  $\rho'$  and  $K'$  denoting the acoustic density and bulk modulus of air, transformation acoustics dictates the required material properties associated with the mapping. These

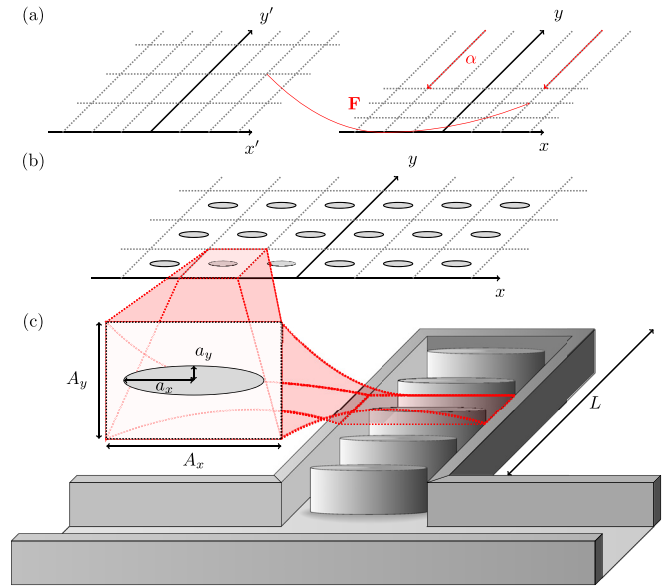


FIG. 1. (a) Visualisation of the transformation on the  $xy$ -plane from the uniform virtual space onto physical space used to obtain the required material properties. (b) The effective properties associated with the physical “stretched” space are realised by the employment of rigid elliptical cylinders placed on a rectangular lattice as is illustrated here together with the unit cell employed. (c) Illustrating that the microstructure realised in (b) can be employed in the quarter wavelength resonator to halve its length, whilst ensuring that it operates at the same frequency.

required properties take the form of an anisotropic density with components  $\rho_x^*$  and  $\rho_y^*$  and a scalar bulk modulus  $K^*$  (see [supplementary material](#)). Note that we do not concern ourselves with matching the required density in the  $z$ -direction and so disregard any stretch or confinement in the  $z$ -direction; this will lead to an impedance mismatch that can be quantified through the value of  $\beta$ . With  $\beta = 1$ ,  $\rho_y^*$  is required to be less than  $\rho'$ . This would provide a perfect impedance match but naturally raises fabrication issues associated with acoustic propagation in air. Employing  $\beta > 1$  allows an increase in  $\rho_y^*$ , above  $\rho'$ , and therefore ensures more straightforward fabrication but with a slight impedance mismatch. This approach was suggested by Popa *et al.*<sup>19</sup> in the context of the two-dimensional acoustic ground cloak.

In order to realise the required properties, we employ an array of rigid cylinders with an elliptical cross-section arranged on a rectangular lattice. The ellipse has semi-axes  $a_x$  and  $a_y$ , and the array has lattice spacings of  $A_x$  and  $A_y$  along the  $x$  and  $y$  directions, respectively, as shown in Figs. 1(b) and 1(c). Parameters need to be chosen such that the effective material properties of this inhomogeneous medium, which we shall denote as  $\rho_x^{\text{eff}}$ ,  $\rho_y^{\text{eff}}$ , and  $K^{\text{eff}}$ , match those of the required material arising from transformation acoustics, i.e.,  $\rho_x^* = \rho_x^{\text{eff}}$ ,  $\rho_y^* = \rho_y^{\text{eff}}$ , and  $K^* = K^{\text{eff}}$ , but in general, this is not possible for the application considered here. We therefore follow a similar approach to Popa *et al.*<sup>19</sup> and minimise the difference between the material properties of a structure we can readily fabricate and those of the required material with  $\beta$  as an additional parameter associated with impedance mismatch. The problem therefore possesses five parameters: two belonging to the transformation,  $\alpha$  and  $\beta$ , and three belonging to the elliptical-microstructure,  $a_x$  and  $a_y$ , the semi-axes, and  $A = A_x/A_y$  the relative spacing. The

lengthscale  $A_y$  is the size of the microstructure, which is required to be much smaller than the propagating wavelengths of interest for homogenization theory to be valid.

The effective properties of the array are determined by the integral equation method of homogenization,<sup>16,17</sup> the benefit of which is an explicit form for the effective properties in terms of the parameters of the problem. For fast optimization, we use the simplest version of the method to determine the domain in which the optimal properties will reside. We then use Comsol Multiphysics to further explore this local region of parameter space identified by the homogenization method, including viscous and thermal losses to provide an optimal parameter choice (see [supplementary material](#)).

Using this approach, we minimise the difference between the effective properties of a medium with a given ellipse of fixed semi-axes and those required by a general transformation over the transformation parameters and relative lattice spacing. We find an optimal microstructure yielding  $\alpha = 0.5$ , with  $a_x = 0.47A_x$ ,  $a_y = 0.05A_y$ , and  $A_x = 2.67A_y$ . This gives effective densities of approximately 1.1 and 5.0 times the density of air in the  $x$  and  $y$  directions, respectively; the bulk modulus is approximately 1.1 times that of air also. Hence, in the  $y$  direction, the speed of sound (given by  $\sqrt{K^{\text{eff}}/\rho_y^{\text{eff}}}$ ) is reduced to approximately half that of air, while in the  $x$  direction, the speed of sound is approximately matched to that of air. It remains to choose a value for  $A_y$ , which should be significantly smaller than the incident wavelength in order for the homogenization theory to be valid. However, if we take  $A_y$  too small, we will greatly increase the surface area of the embedded microstructure and promote viscous and thermal losses within our effective material, which may not be ideal (see [supplementary material](#) for all details of the methodology of parameter optimization). The selection of this final constant is application dependent. With the parameters as chosen above, we term this a “near-miss” microstructure, referring to its ability to closely match the required material properties from transformation acoustics.

At this point, it is worth noting that transformation acoustics is not necessarily required in order to design the metamaterial, since one could in principle immediately write down the required slow sound speed and near-impedance match criteria and then use microstructure/homogenization in order to realise these properties as described above. However, transformation acoustics provides a formal framework allowing for the design of complex metamaterial properties that would not be possible with “ad-hoc” approaches. The procedure outlined above can therefore be used to manipulate sound in more complex ways by employing more elaborate transformations coupled with associated “near-miss” microstructures.

Having optimised the microstructure to effectively reduce sound speed inside the inhomogeneous medium to half that of air, we now employ this medium in the application to a QWR of length  $L$ , as illustrated in Fig. 1(c). Without the microstructure, the QWR will naturally attenuate waves of wavelength approximately  $\lambda = 4L$  corresponding to a frequency of attenuation  $f = c/\lambda$ , where  $\lambda$  is the wavelength of the incident wave in air and  $c$  the speed of sound in air. Here however, by employing the slow sound

medium with near impedance matching, for the same length  $L$ , we achieve  $f = c/2\lambda$ , hence deepening the resonant frequency significantly and effectively creating an “eighth wavelength resonator.” An alternative way of viewing this is to say that with the microstructured resonator, one can attenuate waves of the same frequency with a resonator that is half the length of a standard QWR, thus creating a space-saving resonator device.

Employing a 3D printer, we fabricated a microstructured resonator of total length  $L = 40$  mm, with cell height  $A_y = 10$  mm and with the other parameters as detailed above and with dimensions provided in Fig. 2, for experimental testing in a standard two port experiment.<sup>29,30</sup> The material used to fabricate the resonator and cylinders was Accura 25 plastic from 3D Systems, which has a solid density of  $1190 \text{ kg/m}^3$ . Note that this density is three orders of magnitude greater than that of air, and therefore, the acoustically hard boundary condition is assumed to be reasonable. The associated transmission loss in the two port experiment is defined in the standard manner  $TL = 20 \log_{10}(|p_{in}/p_{out}|)$  (where  $p_{in}$  is the total acoustic pressure field prior to the side branch and  $p_{out}$  is the total acoustic pressure field after the side branch), and this is plotted as a function of frequency in

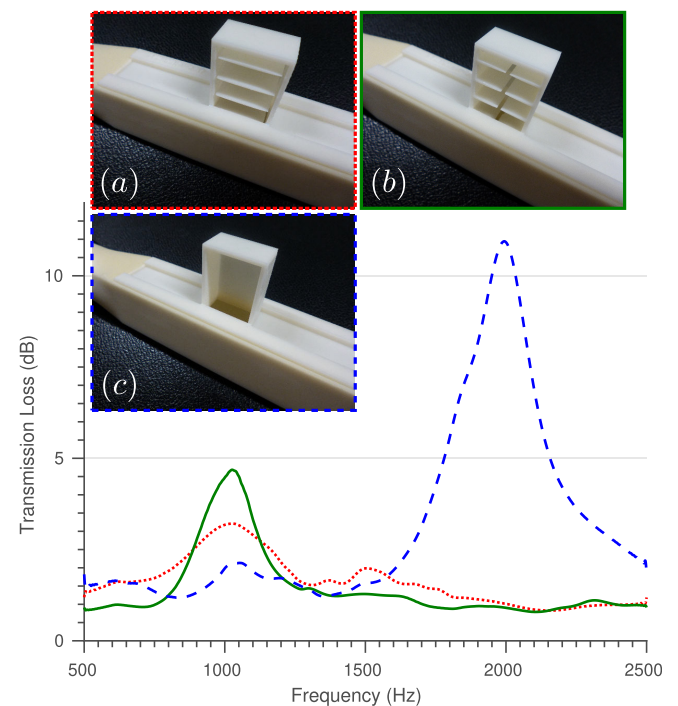


FIG. 2. Experimental results illustrating the transmission loss across three resonant side branches of equal length. Branch (a), corresponding to the dotted red curve, has a microstructure of one ellipse wide with the ellipse centred on the branch centre. Each unit cell is 26.7 mm wide and 10 mm tall; the ellipse has a major semi-axis of 12.5 mm and a minor semi-axis of only 0.5 mm. There are four unit cells within the side branch making the side branch 40 mm long with an opening of 26.7 mm. Branch (b), corresponding to the solid green curve, once again has a microstructure one ellipse wide; however, now the ellipses are centred on the branch walls. All dimensions are as in the previous case, and the unit cell is simply shifted. Branch (c), corresponding to the dashed blue curve, is a standard air filled resonator for comparison. In all cases, the duct and side-branch are 30 mm and 18 mm deep, respectively. The data shown here have had noise removed using a fast Fourier transform. The halving of the resonant frequency in the case of a microstructured resonator is clearly visible.

Fig. 2. The data shown have been post-processed using a Fourier transform to remove noise for clarity. Experiments were carried out at 20 °C with the associated speed of sound in air as 343 m/s. The dashed blue curve in the figure shows the transmission loss due to an ordinary air filled QWR; we see a large amount of transmission loss at the predicted frequency, corresponding to a wavelength of approximately four times the length of the QWR. For the case of a single ellipse across the width of a side-branch of the same length (dotted red curve), we clearly see the decrease in resonant frequency by a factor of a half as predicted, although as may be observed, the magnitude of the loss is decreased somewhat. This reduction is associated with not only impedance mismatch between the slow sound microstructure and that of air but also viscous and thermal losses in boundary layers in the narrow air gaps of the microstructure between the walls of the side branch and the ellipses. This loss mechanism results in less energy returning to the resonator neck in order to destructively interfere with the incoming wave at the resonant frequency. With this in mind, a further resonator was printed with the microstructure shifted by a half cell width in order to have one wider air gap along the centre of the resonator rather than two narrower air gaps at the resonator walls. This offset microstructure gives significant gain in transmission loss (solid green curve), and it should be noted that the level of loss achieved would result in an audible difference in the tone level. Photographs of the cross-sections of both of the microstructured resonators are provided in Fig. 3.

In conclusion, we have shown how to design and construct a slow sound material that is nearly impedance matched to air. Transformation acoustics is employed to derive the required material properties due to our prescribed coordinate stretch. Following this, the integral equation method of homogenization was pivotal in yielding approximate analytical formulae for the material properties of an array of elliptical cylinders on a rectangular lattice. These formulae allowed for fast and accurate optimization of the microstructure in order to best fit the required slow sound

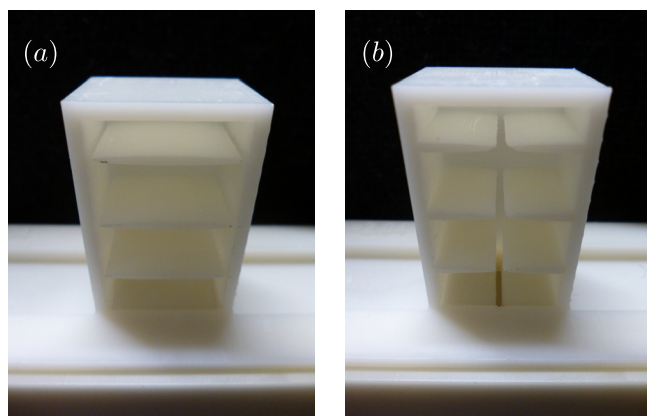


FIG. 3. Cross-section of side branches employed to half the resonant frequency of the resonator. Cylinders with high aspect ratio ellipses are employed in two different configurations. In (a), full cylinders are centred along the middle of the branch, with a narrow gap down each side. In (b), cylinders are halved and attached to the left and right walls of the resonator, with a wider gap down the middle. The latter approach reduces loss and thus enhances the resonance.

properties. This approximation was then used as a starting point for numerical simulations, vastly narrowing down the search space in which to find an optimal configuration and including the effects of viscous and thermal losses. The developed slow sound material was used inside a quarter wavelength resonator in order to halve its resonant frequency or alternatively to halve the length of a resonator required to attenuate a given tone. This specific application has the potential for significant industrial impact, specifically improved sound quality with a reduced form factor (patent pending<sup>31</sup>) while the theoretical ideas and associated universal broadband microstructure have widespread potential for exploitation in a breadth of acoustic devices in the future.

See [supplementary material](#) for details of the theory associated with transformation acoustics, homogenization, and optimization of the microstructure.

W.D.R. thanks the EPSRC and Dyson for funding via a KTN Industrial CASE Ph.D. Studentship, W.J.P. is grateful to the EPSRC for his fellowship under Grant No. EP/L018039/1, and I.D.A. contributed whilst in receipt of a Royal Society Wolfson Research Merit Award and latterly under EPSRC Grant No. EP/K033208/I.

<sup>1</sup>S. A. Cummer, J. Christensen, and A. Alù, “Controlling sound with acoustic metamaterials,” *Nat. Rev. Mater.* **1**, 16001 (2016).

<sup>2</sup>S. A. Cummer and D. Schurig, “One path to acoustic cloaking,” *New J. Phys.* **9**(3), 45 (2007).

<sup>3</sup>D. Torrent and J. Sánchez-Dehesa, “Acoustic cloaking in two dimensions: A feasible approach,” *New J. Phys.* **10**(6), 063015 (2008).

<sup>4</sup>S. Zhang, L. Yin, and N. Fang, “Focusing ultrasound with an acoustic metamaterial network,” *Phys. Rev. Lett.* **102**(19), 194301 (2009).

<sup>5</sup>J. Christensen and F. J. G. de Abajo, “Anisotropic metamaterials for full control of acoustic waves,” *Phys. Rev. Lett.* **108**(12), 124301 (2012).

<sup>6</sup>N. Kaina, F. Lemoult, M. Fink, and G. Lerosey, “Negative refractive index and acoustic superlens from multiple scattering in single negative metamaterials,” *Nature* **525**(7567), 77–81 (2015).

<sup>7</sup>J. P. Groby, W. Huang, A. Lardeau, and Y. Aurégan, “The use of slow waves to design simple sound absorbing materials,” *J. Appl. Phys.* **117**(12), 124903 (2015).

<sup>8</sup>Z. Liang and J. Li, “Extreme acoustic metamaterial by coiling up space,” *Phys. Rev. Lett.* **108**(11), 114301 (2012).

<sup>9</sup>Z. Liang, T. Feng, F. L. Shukin Lok, K. B. Ng, C. H. Chan, J. Wang, S. Han, S. Lee, and J. Li, “Space-coiling metamaterials with double negativity and conical dispersion,” *Sci. Rep.* **3**, 1614 (2013).

<sup>10</sup>Y. Xie, B. I. Popa, L. Zigoneanu, and S. A. Cummer, “Measurement of a broadband negative index with space-coiling acoustic metamaterials,” *Phys. Rev. Lett.* **110**(17), 175501 (2013).

<sup>11</sup>T. Frenzel, J. David Brehm, T. Bückmann, R. Schittny, M. Kadic, and M. Wegener, “Three-dimensional labyrinthine acoustic metamaterials,” *Appl. Phys. Lett.* **103**(6), 061907 (2013).

<sup>12</sup>X. Zhu, K. Li, P. Zhang, J. Zhu, J. Zhang, C. Tian, and S. Liu, “Implementation of dispersion-free slow acoustic wave propagation and phase engineering with helical-structured metamaterials,” *Nat. Commun.* **7**, 11731 (2016).

<sup>13</sup>A. Climente, D. Torrent, and J. Sánchez-Dehesa, “Sound focusing by gradient index sonic lenses,” *Appl. Phys. Lett.* **97**(10), 104103 (2010).

<sup>14</sup>“Acoustic metamaterials,” in *Acoustic Metamaterials: Negative Refraction, Imaging, Lensing and Cloaking*, edited by R. V. Craster and S. Guenneau (Springer Science+Business Media, 2012), Vol. 166, Chap. 3.

<sup>15</sup>A. N. Norris, “Acoustic cloaking theory,” *Proc. R. Soc. A* **464**(2097), 2411–2434 (2008).

<sup>16</sup>D. Joyce, W. J. Parnell, R. C. Assier, and I. D. Abrahams, “An integral equation method for the homogenization of unidirectional fibre-reinforced media; antiplane elasticity and other potential problems,” *Proc. R. Soc. A* **473**(2201), 20170080 (2017).

- <sup>17</sup>W. J. Parnell and I. D. Abrahams, "A new integral equation approach to elastodynamic homogenization," *Proc. R. Soc. A* **464**(2094), 1461–1482 (2008).
- <sup>18</sup>S. Zhang, C. Xia, and N. Fang, "Broadband acoustic cloak for ultrasound waves," *Phys. Rev. Lett.* **106**(2), 024301 (2011).
- <sup>19</sup>B. I. Popa, L. Zigoneanu, and S. A. Cummer, "Experimental acoustic ground cloak in air," *Phys. Rev. Lett.* **106**(25), 253901 (2011).
- <sup>20</sup>L. Zigoneanu, B. I. Popa, and S. A. Cummer, "Three-dimensional broadband omnidirectional acoustic ground cloak," *Nat. Mater.* **13**, 352–355 (2014).
- <sup>21</sup>W. Lu, H. Jia, Y. Bi, Y. Yang, and J. Yang, "Design and demonstration of an acoustic right-angle bend," *J. Acoust. Soc. Am.* **142**(1), 84 (2017).
- <sup>22</sup>L. E. Kinsler, A. R. Frey, A. B. Coppens, and J. V. Sanders, *Fundamentals of Acoustics*, 4th ed. (Wiley-VCH, 1999), p. 560.
- <sup>23</sup>S. H. Lee, C. M. Park, Y. M. Seo, Z. G. Wang, and C. K. Kim, "Acoustic metamaterial with negative modulus," *J. Phys.: Condens. Matter* **21**(17), 175704 (2009).
- <sup>24</sup>X. Wang and C. M. Mak, "Wave propagation in a duct with a periodic Helmholtz resonators array," *J. Acoust. Soc. Am.* **131**(2), 1172–1182 (2012).
- <sup>25</sup>N. Fang, D. Xi, J. Xu, M. Ambati, W. Srituravanich, C. Sun, and X. Zhang, "Ultrasonic metamaterials with negative modulus," *Nat. Mater.* **5**(6), 452–456 (2006).
- <sup>26</sup>S. H. Lee, C. M. Park, Y. M. Seo, Z. G. Wang, and C. K. Kim, "Composite acoustic medium with simultaneously negative density and modulus," *Phys. Rev. Lett.* **104**(5), 054301 (2010).
- <sup>27</sup>J. Mei, G. Ma, M. Yang, Z. Yang, W. Wen, and P. Sheng, "Dark acoustic metamaterials as super absorbers for low-frequency sound," *Nat. Commun.* **3**, 756 (2012).
- <sup>28</sup>N. Jiménez, W. Huang, V. Romero-García, V. Pagneux, and J. P. Groby, "Ultra-thin metamaterial for perfect and quasi-omnidirectional sound absorption," *Appl. Phys. Lett.* **109**(12), 121902 (2016).
- <sup>29</sup>ASTM E2611-09, *Standard Test Method for Measurement of Normal Incidence Sound Transmission of Acoustical Materials Based on the Transfer Matrix Method* (ASTM, 2009).
- <sup>30</sup>M. L. Munjal, *Acoustics of Ducts and Mufflers with Application to Exhaust and Ventilation System Design* (John Wiley and Sons, 1987).
- <sup>31</sup>The University of Manchester, "Apparatus for modifying acoustic transmission," U.K. patent GB1709986.2 (22 June 2017).